Facial Deblur Inference using Subspace Analysis for Recognition of Blurred Faces

Masashi Nishiyama, Abdenour Hadid, Hidenori Takeshima, Jamie Shotton, Tatsuo Kozakaya, Osamu Yamaguchi

Abstract— **This paper proposes a novel method for recognizing faces degraded by blur using deblurring of facial images. The main issue is how to infer a Point Spread Function (PSF) representing the process of blur on faces. Inferring a PSF from a single facial image is an ill-posed problem. Our method uses learned prior information derived from a training set of blurred faces to make the problem more tractable. We construct a feature space such that blurred faces degraded by the same PSF are similar to one another. We learn statistical models that represent prior knowledge of predefined PSF sets in this feature space. A query image of unknown blur is compared with each model and the closest one is selected for PSF inference. The query image is deblurred using the PSF corresponding to that model, and thus ready for recognition. Experiments on a large face database (FERET) artificially degraded by focus or motion blur show that our method substantially improves the recognition performance compared to existing methods. We also demonstrate improved performance on real blurred images on FRGC 1.0 face database. Furthermore, we show and explain how combining the proposed facial deblur inference with the local phase quantization (LPQ) method can further enhance the performance.**

Index Terms— **Face Recognition, Inference, Point Spread Function, Deblur**

I. Introduction

DUE to its many potential applications, face recognition has become one of the most active topics in computer vision research [1]. However, despite the significant progress in the last decade, the design of recognition algorithms that are effective over a wide range of viewpoints, occlusions, aging of subjects and complex outdoor lighting is still a major area of research. While there is a significant number of works addressing these issues, problems caused by image degradations due to other factors such as blur, noise and sampling are mostly overlooked. This is particularly surprising as such image degradations also significantly affect the performance of face recognition systems and are often present in images and videos in real-world applications such as watch-list monitoring and video surveillance. Only recently has research community started to look at facial image degradations e.g. through facial denoising [2]. The focus of this paper is therefore coping with blur and, in particular, automatic deblurring of face images for enhancing the recognition performance.

Blur affects the appearance of faces in images, causing two main problems for face recognition: (i) the facial appearance of an individual changes drastically due to blur as Figure 1 (a) and (b) depict; and (ii) different individuals tend to appear more similar when blurred (for example, the difference in the appearance between the two blurred faces in Figure 1 (b) and (d) is much smaller than that between the corresponding sharp faces in Figure 1 (a) and (c)).

A few existing methods attempt to handle these problems. However, they are not yet satisfactory when facing the significant amount of blur that is common in many real-world settings.

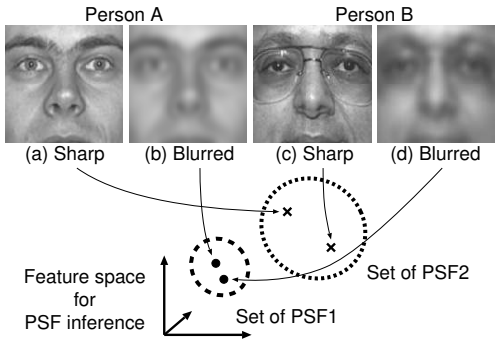

Fig. 1. Variation in facial appearance caused by blur. We construct a new frequency magnitude-based feature space in which faces with similar level of blur are close to each other, regardless of identity. These sets are used to find an appropriate PSF to deblur query images for accurate face recognition.

For instance, Stainvas & Intrator [3] match a query image to artificially blurred copies of the original sharp target images registered for identification. The method can alleviate the first problem of dissimilarity caused by blur, but the second problem of similarity remains. Moreover, the target images may already be blurred themselves. Our approach is based on *removing* the blur from facial appearances using blind image deconvolution [4]. The deblurred images can then be used to perform more robust recognition. Obviously, such an approach can solve both problems (i) and (ii) simultaneously, but requires a Point Spread Function (PSF) that represents the blurring process.

In the field of blind image deconvolution, many methods have been proposed for deblurring from a single image [5]. For instance, Chan and Wong [6] simultaneously infer a PSF and deblur an image using total variation regularization. Other methods attempt to model the smoothness of intensity changes around edges. A PSF is inferred using information derived from this smoothness using the variation of Gaussian scale [7] [8], wavelet coefficient [9] [10], the summation of image derivatives [11], or alpha values representing the object boundary transparency [12]. These methods have to solve an ill-posed problem because they do not adequately exploit the prior knowledge of the image content, and so the quality of the deblurred image using an inferred PSF is often poor. As our experiments will reveal, the deblurred images using these methods are insufficient for accurate face recognition. Yuan et al. [13] and Ancuti et al. [14] infer a PSF using multiple images captured from the same scene. This setting limits face recognition applications. Fergus et al. [15] infer a PSF using heavy-tailed natural image priors, but these priors are very generic and so fairly weak, and the PSF inference is computationally expensive. It appears then that the majority of previous methods for blind image deconvolution use the smoothness of intensity changes around edges to infer the PSF from a single image without prior knowledge of the image contents. These methods

thus often infer a poor quality PSF as it is difficult to distinguish between blurred edges and smooth object surfaces.

Our idea is to exploit prior knowledge of how facial appearances are changed by blur. We thus introduce a new method called FAcial DEblur INference (FADEIN) for inferring PSFs using learned statistical models of the variation in facial appearance caused by blur. In our method, we define a representative set of PSFs for a particular application during training. We artificially blur the sharp training images for each PSF in the set and use them to build a model of facial appearance under that PSF. The method infers a PSF by comparing the query image (with unknown identity and amount of blur) to each model during testing.

A. Overview of FADEIN

We briefly describe the overview of our FADEIN algorithm. We map blurred images to a feature space for learning statistical models. Simply vectorizing the images does not generalize well for the feature space, since the vectorized images are not clearly separated and yields in poor performance as our experiments in Section III show. We instead design a new 'magnitude-based feature space' in the frequency domain, as illustrated in Figure 1, in which the variation of facial appearance caused by blur is larger than the variation of facial appearance between individuals. Faces blurred by the same PSF are similar in the new feature space. We learn the statistical models by approximating each set as a low-dimensional linear subspace using principal component analysis (PCA). We compare query images to each subspace during testing. The most similar subspace gives an accurate inferred PSF that is used to deblur the query image. The resulted image can then be fed to a standard face recognition algorithm. Our extensive experiments on real and artificially blurred face images show high PSF inference and significant face recognition performance improvements in comparison to existing methods.

B. Extension of FADEIN

The preliminary results of this research have been published in [16]. In this article, we provide improved results including a more thorough investigation and extended experimental evaluation of the algorithm.

We also take the following method into consideration. Recently, Ahonen et al. [17] proposed another interesting approach to the problem of recognizing blurred faces. Instead of performing deblurring, the authors aimed to directly derive blur invariant features from the original face images using the phase information in the frequency domain. The method, called Local Phase Quantization (LPQ), showed promising results. In our extended evaluation, we compare our proposed facial deblur inference against the LPQ approach and demonstrate the superiority of our proposed approach. Furthermore, we describe a combined scheme exploiting the advantages of both methods for further enhancing the face recognition performance.

The rest of this paper is organized as follows. Section II describes our method for PSF inference, and Section III demonstrates its effectiveness through extensive experiments and analysis. We summarize our contributions and conclude in Section IV.

II. Facial deblur inference

In this section we present our new approach (FADEIN) for inferring PSFs using learned statistical models of the variation in facial appearance caused by blur. The degradation process caused by blur is defined as

$$\mathbf{g} = H\mathbf{f} + \mathbf{n} \ , \tag{1}$$

where vector $\mathbf{g}$ represents the blurred image $g(u, v)$, matrix H the PSF, vector $\mathbf{f}$ the original sharp image, and vector $\mathbf{n}$ the noise. Equation (1) represents an explicit appearance model for blur. Note that $\mathbf{g}$ and $\mathbf{f}$ consist of only the facial region given by a face detector. Blur is not a major problem to face detection as the existing method [18] can detect small faces even at 15×15 pixels. Figure 3 shows facial regions detected from blurred images.

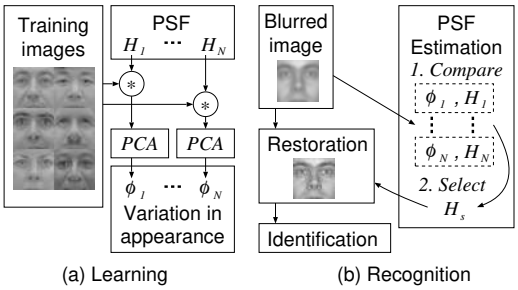

Fig. 2. FADEIN comprises two steps: (a) learning statistical models of facial blur appearance, and (b) using these models to recognize individuals in query images of unknown blur.

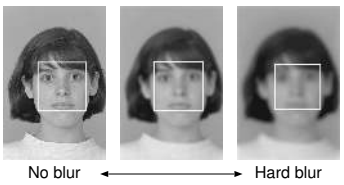

Fig. 3. Examples of detected faces from blurred images using the face detector proposed in [18].

If the PSF H and noise $\mathbf{n}$ are known, a sharp image $\mathbf{f}$ can be exactly recovered from the blurred image $\mathbf{g}$. Our work focuses on accurately inferring a PSF H from a blurred facial image $\mathbf{g}$, though we also compare in our experiments how, given our inferred PSF, two existing deblurring methods cope with the noise.

As illustrated in Figure 2, our approach consists of first learning statistical models of facial blur appearance and then using these models to recognize individuals in query images of unknown blur.

Let us assume that a representative fixed set $\Omega = \{H_i\}_{i=1}^{N}$ of N PSFs are constituted as described in [19]. These PSFs are chosen for a particular application. We represent statistical models for PSF inference as subspaces in the frequency magnitude-based feature space (see Section II-A). We denote a set of statistical models as

$$\Phi = \{ \ (H_i \ , \ \phi_i) \ \}_{i=1}^{N} \ , \tag{2}$$

where ϕ_i represents the subspace modeling the variation in facial appearance induced by PSF H_i. We learn subspaces ϕ_i from a set of M training images $\Psi = \{\mathbf{f}'_k\}_{k=1}^{M}$. A training image $\mathbf{f}'_k$ is a sharp image artificially blurred by each H_i to learn the subspace ϕ_i (see Section II-B). Note that the subjects in Ψ can be completely different to ones for identification. This means that the training images for PSF inference do not depend on the target images registered for identification. The method we are proposing in this article not only overcomes both problems cited in Section I but

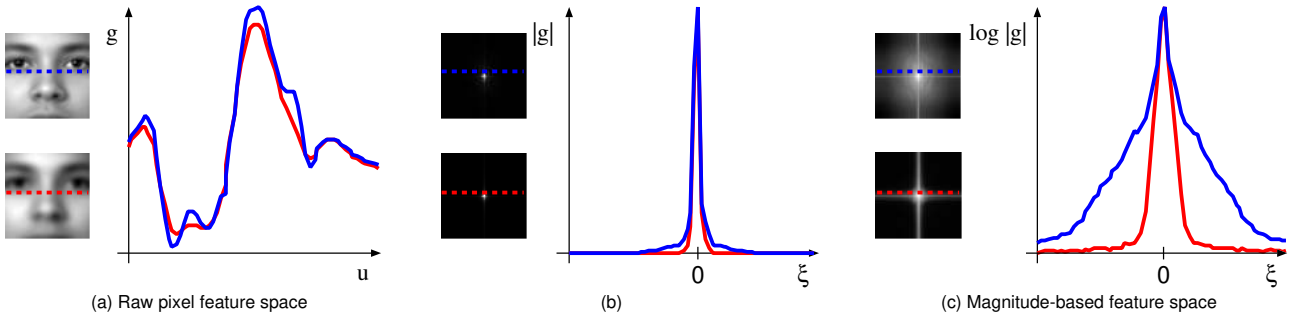

(a) Raw pixel feature space (b) (c) Magnitude-based feature space

Fig. 4. Comparison of feature vectors. The blue curves are feature vectors generated from the top-left sharp image and the red curves are ones generated from the bottom-left blurred image. The average of images of 200 persons is shown. The vectors in our feature space (c) are much more clearly separated than in (a) using raw pixels. (a) One scan-line through a simple vectorization of the image. (b) One row of the 2D Fourier transform of the images. (c) The same row after taking logarithms. The transformations create our feature space. The horizontal axis of (a) represents dashed lines in the face images. The ones of (b), (c) represent frequency on dashed lines in the Fourier domain, with low frequency in the center and higher frequencies further away from the center.

also needs only a single target example and works even for real-life capture settings where the target images are blurred.

A query image $\mathbf{g}$ of unknown blur and identity is compared to each subspace using the subspace method [20]. This method is easy to implement and gives an accurate and stable similarity measure (see Section II-C). The closest subspace ϕ_s is selected and the corresponding PSF H_s is the result of our PSF inference. The query image $\mathbf{g}$ is deblurred using H_s (see Section II-D), and finally identification of the deblurred image is performed.

A. Frequency magnitude-based feature space

We construct a feature space that is sensitive to the appearance variations of different blurs but insensitive to the difference between individuals. We base the feature space on frequency domain amplitude, because of the phenomenon that high-frequency amplitudes for blurred images become smaller than those for sharp images [21]. Since we want a feature space invariant to identity, we deliberately ignore phase information (note that, without blur, phase information is, of course, a good feature for face recognition [22]).

Inferring a PSF using frequency domain amplitude is a well-known technique [19], [23]–[25]. The method in [19] selects a PSF from a representative fixed set Ω using amplitude of a sharp image and noise. But, it is difficult to correctly estimate these amplitudes from the blurred image because the sharp image is unknown. Other methods [23]–[25] use the relationship between PSF parameters and the positions of the zero crossings of amplitude. However, detecting these positions is difficult for real blurred images because the zero crossings are affected by the noise amplitude. Our method instead uses the whole frequency amplitude domain for constructing the feature space. The variation caused by noise is included in the subspaces ϕ_i learned in our feature space by adding noise to training images (see Section II-B).

We emphasize discriminative high-frequency amplitude to improve the PSF inference accuracy. Our method first transforms a blurred image $g(u, v)$ in the space domain to a feature image $x(\xi', \eta')$ as

$$x(\xi', \eta') = [\ C(|g(\xi, \eta)|)\ ] \downarrow , \tag{3}$$

where $g(\xi, \eta)$ is the 2D Fourier transform of $g(u, v)$, $|\ |$ takes the amplitude, C takes dynamic range compression, and $[\ ] \downarrow$ represents downsampling. Dynamic range compression is performed to emphasize high-frequency values because non-discriminative low-frequency values are much larger than discriminative high-frequency values. For the function C, we simply take logarithms that shift from a large value to a small value while maintaining order relation. Downsampling helps reduce noise and accelerate subspace learning. Bilinear interpolation is used for downsampling. We choose the procedures C and $[\ ] \downarrow$ from the viewpoints of computation time and inference accuracy. The feature vector $\mathbf{x}$ is generated by raster scanning $x(\xi', \eta')$. Finally, as preprocessing for the subspace method, vector $\mathbf{x}$ is normalized so that $\|\mathbf{x}\|_2 = 1$.

Figure 4 compares feature vectors generated from a sharp image and its blurred version. The vectors in Figure 4 (a) to (d) are the outputs of each step in Equation (3) and the normalization. Note that the waveforms of the vectors in Figure 4 (a) are almost the same, but the difference between sharp and blurred images appears most cleanly in our feature space in Figure 4 (d).

Further, Figure 5 uses PCA to visualize two feature spaces containing images blurred by three different PSFs. Raw pixel based feature space (center) directly vectorizes the blurred facial images. Observe that our frequency magnitude-based feature space (right) gives sets that are much better separated. Our experiments below compare these two feature spaces and confirm that our feature space gives more accurate PSF inference and face recognition.

B. Learning subspaces

We generate subspaces for the statistical models to represent sets in the feature space. Training images are blurred by applying each PSF H_i to sharp training images $\mathbf{f}'_k$ in a training set Ψ as $\mathbf{g}'_{ik} = H_i \mathbf{f}'_k + \mathbf{n}'$, where $\mathbf{n}'$ is the noise that we assume to be white Gaussian.

Next, we apply PCA to blurred training images $\{\mathbf{g}'_{ik}\}_{k=1}^{M}$ in our feature space, as follows. Having transformed image $\mathbf{g}'_{ik}$ to feature vector $\mathbf{x}'_{ik}$, the correlation matrix [26] is defined as $A_i = \frac{1}{M}\sum_{k=1}^{M} \mathbf{x}'_{ik}(\mathbf{x}'_{ik})^{\mathrm{T}}$. Note that the mean vector of $\{\mathbf{x}'_{ik}\}_{k=1}^{M}$ is not subtracted for the correlation matrix because our implementation of the subspace method uses an angle for similarity measure (see Equation (4)). Eigenvectors and eigenvalues of the correlation matrix A_i are calculated. The first D eigenvectors, sorted by decreasing eigenvalue, form the basis vectors of the subspace $\phi_i = \{\mathbf{b}_{ij}\}_{j=1}^{D}$. The low-dimensional subspace spanned by the basis vectors ϕ_i is defined by maximizing the variance of training feature vectors $\{\mathbf{x'}_{ik}\}_{k=1}^{M}$ in this subspace.

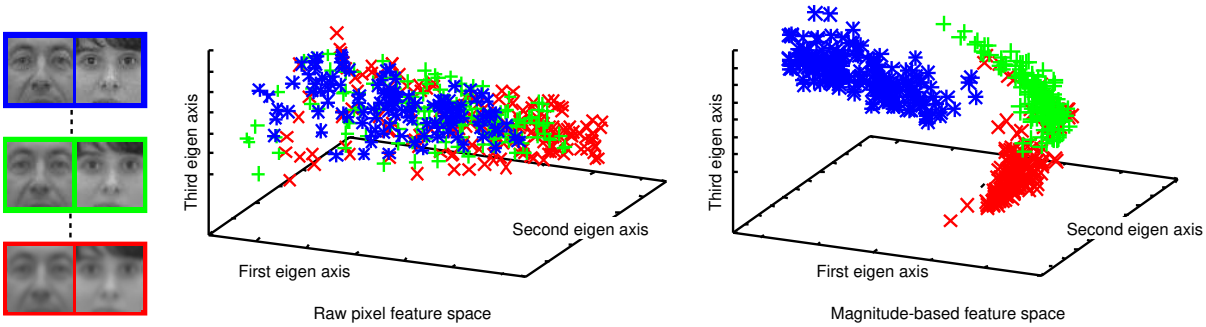

Fig. 5. Visualization of sets in two feature spaces. Artificially blurred facial images (left) are vectorized either directly (center, raw pixels) or using the frequency domain amplitude (right, our method). Colors represent the particular PSFs used to blur the faces. Our evaluation highlights the importance of the much cleaner separation of the PSF sets using our method.

C. Determining the PSF

Given a blurred query image $\mathbf{g}$ of unknown blur, we find the closest subspace ϕ_s in a set of statistical models Φ as

$$\begin{aligned} s &= \arg\max_i \cos^2\theta_i \\ &= \arg\max_i \sum_{j=1}^{D} (\mathbf{b}_{ij}{}^{\mathrm{T}}\mathbf{x})^2, \end{aligned} \tag{4}$$

where $\mathbf{x}$ is the feature vector of $\mathbf{g}$, θ_i is the angle between vector $\mathbf{x}$ and subspace ϕ_i, and $i \in \{1, \ldots, N\}$. A small angle θ_i indicates that the blurred query image $\mathbf{g}$ is similar to a set of the training images blurred by PSF H_i that generated the subspace. The maximization of $\cos^2\theta_i$ over i thus infers the most appropriate PSF H_s.

D. Restoration

Given PSF H_s, we can then remove blur from the degraded query image $\mathbf{g}$. Simple matrix inverse-based deconvolutions give a poor quality result because of existing noise $\mathbf{n}$ in Equation (1). We thus use the BTV regularization from [27]. The detail of BTV is described in the Appendix of [16]. Deconvolution using the BTV regularization recovers not only a sharp image but also a noiseless image.

III. Experimental Analysis on Face Recognition using Facial Deblur Inference

To demonstrate the effectiveness of FADEIN in recognizing blurred (and also sharp) faces, we performed extensive experiments on two publicly available databases, namely FERET [28] and FRGC 1.0 [29]. We investigate camera focus blur by artificially degrading sharp images. Camera focus blur arises when the camera focal length is not correctly adjusted to the subject. We also investigate camera motion blur that arises when the camera is moved while capturing an image. Furthermore, we test our method on real blurred images. In the experiments with artificial blur, only the face regions are blurred while in the experiments with real blurred images, the entire images are blurred and automatic face detection is used for detecting the facial regions.

Facial deblur inference can be used as preprocessing before feature extraction for face recognition. Thus, it can be used with any traditional face recognition algorithm. In our previous work [16], we evaluated the performance using only raw pixel values as features which are computed by simply raster scanning the deblurred image. For extensive experimentation, this paper considers baseline face recognition techniques for feature extraction from the deblurred images. We use the local binary pattern 'LBP' [30], the eigenfaces 'EF' [31], and the laplacianfaces 'LF' [32]. LBP is a face descriptor which makes histograms derived by counting labels assigned to every pixel. The label of LBP is computed by thresholding the neighborhood of each pixel with the center pixel value. EF is a coefficient vector derived by projecting the deblurred image to a linear subspace computed using PCA. LF is a coefficient vector computed by PCA and locality preserving projections that keeps the local structure of neighborhood samples in the feature space.

Once the features are extracted, we adopt in all our experiments the nearest-neighbor (NN) classifier with the Euclidean distance for face recognition. This choice is motivated by the fact that, in most cases, only one query image per person is available.

Fig. 6. Examples of synthesized images of camera focus blur from the subset 'fb' of FERET. Blurred images (b), (c), (d), and (e) are synthesized from the original image (a) using Gaussian PSFs with given standard deviations σ.

A. PSF inference accuracy

To gain insight into the PSF inference accuracy, we analyzed synthesized images by blurring sharp query faces from FERET database. Sharp faces are blurred by shift-invariant Gaussian PSFs as $H(u,v) = \frac{1}{Z}\exp\left(\frac{-(u^2+v^2)}{2\sigma^2}\right)$, where σ is the standard deviation, and Z is a normalization term as $\int\int H(u,v)dudv = 1$. This PSF is defined in the space domain. White Gaussian noise of 30dB is added to the synthesized images. Examples are shown in Figure 6. The facial images are registered using determined facial feature points. Image $g(u,v)$ is of size 128×128, and downsampled $x(\xi',\eta')$ is of size 64×64. For the representative fixed set Ω of PSFs, we use $N = 18$ PSFs, including 17 Gaussians and 1 'no blur' delta function. The parameters of the Gaussian PSFs are set from $\sigma = 1$ to 9 in increments of 0.5. The database includes three subsets: 'bk', 'fa', and 'fb'. Each subset contains a single image per person. Subset 'bk' is used as training set Ψ to learn the subspaces in a set of statistical models Φ. The dimension of each subspace is $D = 20$. The number of training images is

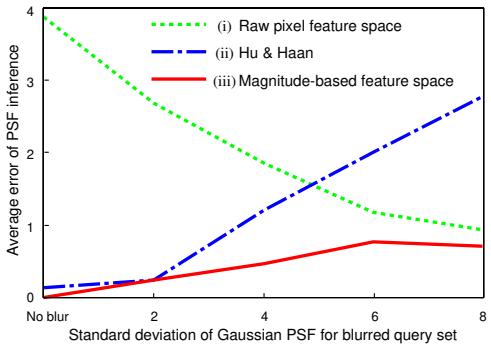

Fig. 7. PSF inference accuracy on FERET of artificially camera focus blur.

TABLE I
RESTORATION PERFORMANCE OF ARTIFICIAL CAMERA FOCUS BLUR.

Method	PSNR
Raw pixel feature space	28.8dB
Hu & Haan [7]	28.4dB
Magnitude-based feature space	30.4dB

$M = 200$. We evaluate inference accuracy on the 1001 images that remain in subsets 'fa' and 'fb' after removing the individuals present in subset 'bk'. The identification target set is 'fa' and the query set is 'fb'.

Figure 7 shows PSF inference accuracy on the query images 'fb'. Average error is defined as $\|\sigma_c - \sigma_s\|_1$ where σ_c is the standard deviation of the PSF used for synthesizing the blurred image (groundtruth), and σ_s is that of the inferred PSF. We compare our method 'magnitude-based feature space' against two alternatives: 'raw pixel feature space' which uses a directly vectorized feature space (cf. Figure 5) and 'Hu & Haan [7]' which estimates the standard deviation of Gaussian PSF from the smoothness of intensity changes around edges. Hu & Haan's method can handle only camera focus blur. From the results in Figure 7, we can clearly see that our PSF inference method performs much better than the alternatives. An interesting anomaly is that the PSF inference accuracy of 'raw pixel feature space' increases with blur. This is probably because increasing the blur reduces variation, which can thus be more adequately represented by a low-dimensional subspace. In Table I, we demonstrate restoration performance in terms of peak signal-to-noise ratio (PSNR) computed between the original image and the deblurred image. We report the average PSNR over different values of σ_c. Our method (30.4dB) performs better than 'raw pixel feature space' method (28.8dB) and Hu & Haan's method (28.4dB).

B. Face recognition performance with and without FADEIN

To analyze the effectiveness of our proposed facial deblur inference (FADEIN), we consider different face recognition methods (EF, LF, and LBP) and compare the recognition results obtained **with** and **without** the use of FADEIN. We evaluated the performance on the target set 'fa' and the artificially blurred query set 'fb' of FERET, which are synthesized using the same settings described in Section III-A.

Figure 8 reports identification accuracy as recognition rate: the probability that a query image is matched to the correct target image of the same individual. We demonstrate the average

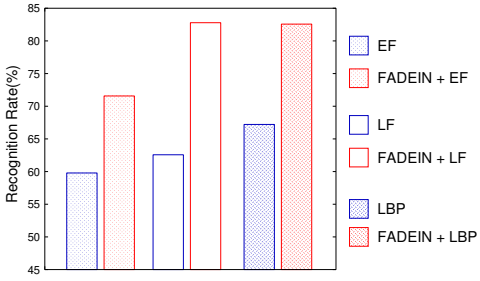

Fig. 8. Identification performance with and without FADEIN on FERET for artificial camera focus blur. Query set are blurred with Gaussian PSF.

TABLE II
IDENTIFICATION PERFORMANCE ON FERET OF ARTIFICIAL CAMERA FOCUS BLUR USING FACE RECOGNITION METHODS CONSIDERING BLUR.

Method	Recognition rate
Hu & Haan [7]	73.4%
LPQ	78.0%
FADEIN	83.4%

recognition rates over different values of σ_c of blur PSFs. It is clearly shown that FADEIN significantly enhances identification performance for all considered methods. For instance, LBP with and without FADEIN yields in identification rates of 82.6% and 67.2%, respectively. FADEIN overcomes the sensitively of LBP to blur which was reported in [17] and also confirmed in our experiments. This very significant gain in recognition performance demonstrates the effectiveness of our proposed facial deblur inference.

In our unoptimized implementation on a single-core 3.4GHz processor, learning in FADEIN takes about 5 minutes and PSF inference takes about 0.5 seconds per image. The BTV regularization [27] takes up to 1.5 seconds per image.

C. Comparing FADEIN-based face recognition to state-of-the-art methods addressing the blur problems

How does our FADEIN-based face recognition technique compare to state-of-the-art methods addressing the blur problem? To investigate this question, we evaluate and compare FADEIN against two alternative methods designed for identifying blurred faces: deconvolution using existing PSF inference before identification and extraction of blur invariant features from blurred faces for identification. For the deconvolution approach, we used the PSF inference of Hu & Haan [7] and the restoration of the BTV regularization. After the deconvolution, we used raw pixel values as features for identification. For the invariant feature approach, we used the local phase quantization (LPQ) method [17] [33]. LPQ works like LBP for extracting face descriptors by assigning quantized label to phase value in the frequency domain. Ahonen et al. have recently adopted LPQ for identifying blurred faces yielding in very good results [17]. Note that LPQ was originally proposed by Ojansivu and Heikkila for blurred texture analysis in [33]. In our approach, we adopted FADEIN for deconvolution and raw pixel values as features. We evaluated the performance on the same database as in Section III-B. The parameters for FADEIN are the same as in Section III-A.

Table II shows identification performance of our method and the two alternatives. We demonstrate the average recognition rates

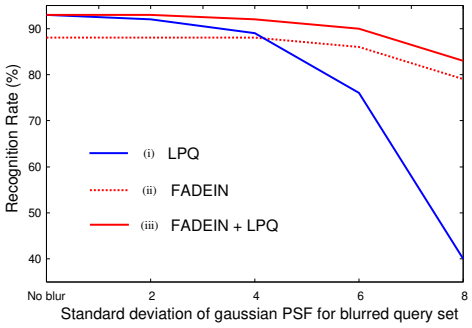

Fig. 9. Identification performance by combining PSF inference methods with LPQ on FERET for artificial camera focus blur.

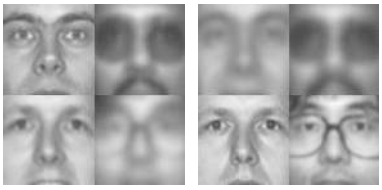

Fig. 10. Examples of images artificially blurred with random standard variation of Gaussian PSF in $(0, 8]$ on FERET. (a) Target images from the subset 'fa'. (b) Query images for the subset 'fb'. Note that both target and query images are blurred to simulate real-life face capture conditions.

on the same setting described in Section III-B. Though LPQ shows better performance compared to Hu & Haan's method (78.0% versus 73.4%), FADEIN significantly outperforms both methods, yielding an identification rate of 83.4%.

D. Combining FADEIN and LPQ

While our FADEIN for face recognition is based on deblurring the face images before recognition, the LPQ method uses a different strategy as it aims at extracting blur invariant features from the original face images using the phase information in the frequency domain. Although the results clearly demonstrate the superiority of FADEIN over LPQ (as shown in Table II and Figure 9), the experiments revealed very interesting properties: while LPQ works very well with small amount of blur and suffers when the amount of blur increases, the FADEIN approach significantly decreases the amount of blur in the face images but uses simple raw pixels as features for recognition. This means that one can look at FADEIN and LPQ as complementary methods for further enhancing the recognition performance. Thus, to exploit the advantages of FADEIN and LPQ, we derived a new approach combining both methods: we extract the LPQ features from the deblurred face images. Figure 9 shows then the results of this combination 'FADEIN + LPQ'. As expected, the combined approach enhances the recognition performance compared to the use of FADEIN and LPQ separately. We also studied other combination schemes such as fusing FADEIN with LPQ and/or LBP at feature level but the results were not better than 'FADEIN + LPQ'.

E. Experiments with different artificial blur settings

1) Random focus blur: We tested identification performance on FERET when the query set images were blurred by an unknown random Gaussian sigma in the range $(0, 8]$. Figure 10 shows

TABLE III
IDENTIFICATION PERFORMANCE OF ARTIFICIAL CAMERA FOCUS BLUR WITH RANDOM STANDARD VARIATION OF GAUSSIAN PSF.

Method	Recognition rate
LPQ	84.0%
Hu & Haan [7] + LPQ	83.8%
FADEIN	82.8%
FADEIN + LPQ	88.3%

TABLE IV
IDENTIFICATION PERFORMANCE FOR ARTIFICIAL CAMERA MOTION BLUR.

Method	Recognition rate
LPQ	59.3%
Yitzhaky & Kopeika [11] + LPQ	49.1%
FADEIN	82.0%
FADEIN + LPQ	82.3%

examples used in this experiment. Some faces are blurred only in target images and other faces are blurred only in query images. Note that facial deblur inference is performed on *both* target and query images. From Table III, an improvement over the other methods by combining our deblurring and LPQ is again evident and consistent performance is demonstrated for unknown blurs that do not precisely coincide with the training PSFs.

2) Camera motion blur: In the second experiment, tests were performed on synthesized images by blurring sharp query faces from FERET using shift-invariant linear motion blur PSFs as $H(u, v) = 1/Z$ if $\|(u, v)\|_2 < b$ and $v = u \tan\theta$, otherwise $H(u, v) = 0$,where b is the length of camera motion, θ is the angle, and Z is a normalization term. White Gaussian noise of 30dB is added to the synthesized images. Identification query images are blurred by the PSF in the range $b = 5, 10, 15, 20$ and $\theta = 0, 0.25\pi, 0.5\pi, 0.75\pi$. Examples are shown in Figure 11. For the representative fixed set Ω of PSFs, we use $N = 41$ PSFs, including $10 \times 4 = 40$ motion blur function and 1 'no blur' delta function. The parameters are set from $b = 2.5$ to 25 in increments of 2.5 and from $\theta = 0$ to 0.75π in increments of 0.25π. The other parameters for learning statistical models are the same as in Section III-A.

Table IV reports average recognition rate. We compare our methods to two alternatives. The first one is LPQ as in Section III-C. While the PSF inference of Hu & Haan [7] cannot be applied because it is only considers focus blur, we instead use the method of Yitzhaky & Kopeika [11]. As Table IV shows, our approaches yield again in significantly better results compared to the two alternatives (LPQ and Yitzhaky & Kopeika's method). The average errors between the correct parameters of blurred query images and the inferred ones using Yitzhaky & Kopeika's method [11] were $b = 6.2, \theta = 0.1$ while FADEIN yielded in significantly better performance ($b = 0.7, \theta = 0.0$).

3) Putting 2 PSF types together: For simultaneously handling both types of blur (out-of-focus and camera motion), we conducted experiments by putting the two types of PSF together. We used 18 PSFs of focus blur described in Section III-A and 40 PSFs of motion blur described in Section III-E.2 to learn the statistical models Φ. Given an unknown PSF image, FADEIN selects a PSF from the $18 + 40 = 58$ PSFs. Target set is no blur

Fig. 11. Examples of synthesized images of camera motion blur from the subset 'fb' of FERET. Blurred images are synthesized from Figure 6 (a) using linear motion blur PSFs with given b, θ.

TABLE V
IDENTIFICATION PERFORMANCE FOR PUTTING 2 PSF TYPES TOGETHER (FOCUS AND MOTION BLURS).

Method	Recognition rate
LPQ	66.6%
FADEIN	79.6%
FADEIN + LPQ	82.9%

'fa' and query set is 'fb' artificially blurred by focus blur (the same setting described in Section III-B) and motion blur (the same one described in Section III-E.2).

Table V reports the average recognition rates over all the query images. The obtained results show that our proposed approach (FADEIN) yields better performance than LPQ. Miss classification rate of the two PSF types (i.e. confusion between motion and focus blurs) was only 1.0%.

F. Evaluation on real blurred face images

The final experiment used real blurred images from FRGC 1.0. We evaluated identification performance in terms of verification rate under the setups 'Exp4' that is evaluated on uncontrolled still query images including blurred faces. Each query set consists of 608 images of 152 individuals. We count that 366 query images are degraded by camera focus blur. Target images are collected under a controlled still condition. A single image is captured per person for target. The number of target images is 152. Figure 12 shows example images from FRGC 1.0. Camera focus blur arises in Figure 12 (b) as the camera focal length is adjusted to the background. The amount of blur in both the target and query images is not constant and is unknown. Note that facial deblur inference is performed on *both* target and query images, since real face target databases already contain considerable focus blur. For the representative fixed set Ω of PSFs, we use $N = 8$ PSFs, including 7 Gaussians and 1 'no blur' delta function. The parameters of the Gaussian PSFs are set from $\sigma = 1$ to 4 in increments of 0.5. Three subsets 'bk', 'fa', and 'fb' in FERET are used as training set Ψ to learn the subspaces in a set of statistical models Φ. The dimension of each subspace is $D = 20$. The number of training images is $M = 2591$.

Fig. 12. Example images from FRGC 1.0. (a) Target image. (b) Query image in Exp4. Real camera focus blur arises in (b).

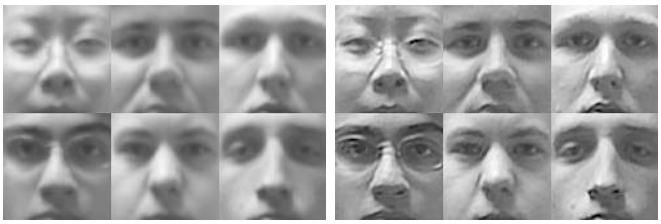

Fig. 13. (a) Example images from FRGC 1.0 with real blur. (b) Faces deblurred using FADEIN.

We show some deblurred images in Figure 13. The deblurred images are sharp compared with the blurred images. We evaluated ROC curves in terms of verification rate and false acceptance rate. As shown in Figure 14, the use of FADEIN for deblurring real face images also enhances the performance of LPQ and outperforms the PSF inference of Hu & Haan [7], confirming our earlier findings. We can also notice in Figure 14 that the performance enhancement using only FADEIN is not as significant as with the artificially blurred faces in the previous experiments e.g. Figure 6. This is mainly due to the fact that these real blurred faces contain less blur than the artificially blurred faces. Figure 15 shows the inferred amount of blur in these real blurred face images. The median value is $\sigma = 2.5$ excluding no blurred faces. With additional blur, we expect much more performance enhancement using FADEIN.

IV. CONCLUSION

We proposed a novel approach for recognizing blurred faces using facial deblur inference. Our algorithm inferred PSF using learned models of facial appearance variation under different amounts of blur. The inferred PSFs were used to sharpen both query and target images. Our extensive experiments on both real and artificially blurred face images demonstrated substantially more accurate PSF inference and face recognition than existing methods. The salient contributions of this paper are the following:

- Learning statistical models of the variation in facial appearance caused by blur to accurately infer PSFs from blurred images.
- A new frequency magnitude-based feature space in which these statistical models are learned. This feature space is designed to emphasize the different appearances of different levels of blur but be invariant to facial identity.
- A demonstration that these statistical models generalize well, maintaining PSF inference accuracy: the models are trained on faces that are completely different to target images for identification.
- A new scheme combining facial deblur inference with LPQ

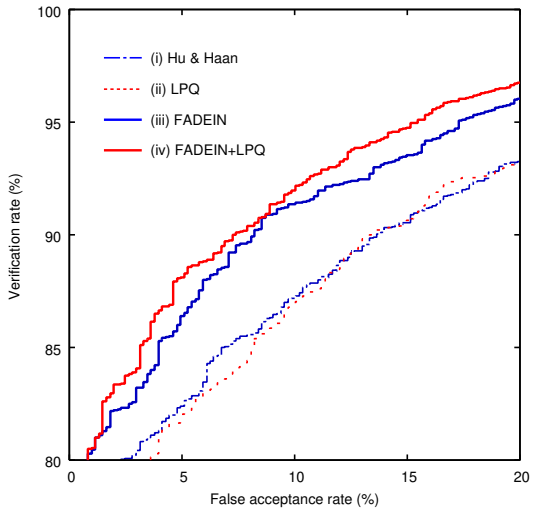

Fig. 14. ROC curves on FRGC 1.0 (real blurred images).

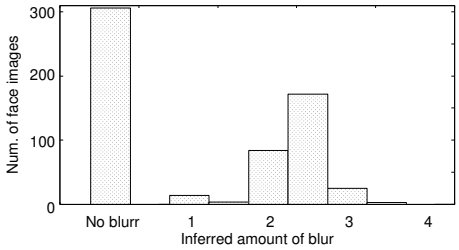

Fig. 15. Histogram of inferred amount of blur on FRGC 1.0.

(which is one of the state-of-the-art methods) is introduced, yielding in excellent results.

We believe that our deblurring method has relevance not only for face recognition, but also for other restricted classes of images, such as recognizing textual character, hand and body postures under blur. However, our method may not work well for other objects consisting of uniform texture, e.g. plaster sphere, plastic cup, and metal fork. Note also that our proposed approach (FADEIN) has not yet been proven for images blurred with multi unknown factors or with severe blur such as camera shake. As future work, we are planning to explore and improve the tolerance of our approach to such factors. A promising direction consists of modeling the PSF inference as a regression problem rather than a classification problem, which is likely to scale better when multiple factors are considered together.

REFERENCES

[1] S. Z. Li and A. K. Jain, *Handbook of Face Recognition*. Springer, 2005.

[2] T. Bourlai, A. Ross, and A. K. Jain, "On matching digital face images against scanned passport photos," *Proc. IEEE Int'l Conf. Biometrics, Identity and Security*, 2009.

[3] I. Stainvas and N. Intrator, "Blurred face recognition via a hybrid network architecture," *Proc. Int'l Conf. Pattern Recognition*, vol. 2, pp. 805 – 808, 2000.

[4] D. Kundur and D. Hatzinakos, "Blind image deconvolution," *IEEE Signal Processing Magazine*, pp. 43 – 64, May 1996.

[5] P. Campisi and K. Egiazarian, *Blind Image Deconvolution : Theory and Applications*. Taylor & Francis, 2007.

[6] T. F. Chan and C.-K. Wong, "Total variation blind deconvolution," *IEEE Trans. Image Processing*, vol. 7, no. 3, pp. 370 – 375, 1998.

[7] H. Hu and G. de Haan, "Low cost robust blur estimator," *Proc. IEEE Int'l Conf. Image Processing*, pp. 617 – 620, 2006.

[8] J. H. Elder, "Local scale control for edge detection and blur estimation," *IEEE Trans. Pattern Analysis and Machine Intelligence*, vol. 20, no. 7, pp. 699 – 716, 1998.

[9] F. Rooms, A. Pizurica, and W. Philips, "Estimating image blur in the wavelet domain," *Proc. Fifth Asian Conf. Computer Vision*, pp. 210 – 215, 2002.

[10] H. Tong, M. Li, H. Zhang, and C.Zhang, "Blur detection for digital images using wavelet transform," *IEEE Proc. Int. Conf. Multimedia and Expo*, vol. 1, pp. 17 – 20, 2004.

[11] Y. Yitzhaky and N. S. Kopeika, "Identification of blur parameters from motion blurred images," *Graphical Models and Image Processing*, vol. 59, no. 5, pp. 310 – 320, 1997.

[12] J. Jia, "Single image motion deblurring using transparency," *Proc. IEEE Conf. Computer Vision and Pattern Recognition*, pp. 1 – 8, 2007.

[13] L. Yuan, J. Sun, L. Quan, and H. Y. Shum, "Image deblurring with blurred/noisy image pairs," *ACM Trans. Graphics*, vol. 26, no. 3, pp. 1 – 10, 2007.

[14] C. Ancuti, C. O. Ancuti, and P. Bekaert, "Deblurring by matching," *Computer Graphics Forum*, vol. 28, no. 2, pp. 619 – 628, 2009.

[15] R. Fergus, B. Singh, A. Hertzmann, S. T. Roweis, and W. T. Freeman, "Removing camera shake from a single photograph," *ACM Trans. Graphics*, vol. 25, no. 3, pp. 787 – 794, 2006.

[16] M. Nishiyama, H. Takeshima, J. Shotton, T. Kozakaya, and O. Yamaguchi, "Facial deblur inference to improve recognition of blurred faces," *Proc. IEEE Conf. Computer Vision and Pattern Recognition*, pp. 1115–1122, 2009.

[17] T. Ahonen, E. Rahtu, V. Ojansivu, and J. Heikkila, "Recognition of blurred faces using local phase quantization," *Proc. Int'l Conf. Pattern Recognition*, pp. 1 – 4, 2008.

[18] T. Mita, T. Kaneko, B. Stenger, and O. Hori, "Discriminative feature co-occurrence selection for object detection," *IEEE Trans. Pattern Analysis and Machine Intelligence*, vol. 30, no. 7, pp. 1257–1269, 2008.

[19] A. E. Savakis and H. J. Trussell, "Blur identification by residual spectral matching," *IEEE Trans. Image Processing*, vol. 2, no. 2, pp. 141 – 151, 1993.

[20] S. Watanabe and N. Pakvasa, "Subspace method of pattern recognition," *Proc. Int. Joint Conf. Pattern Recognition*, pp. 25 – 32, 1973.

[21] R. C. Gonzalez and R. E.Woods, *Digital Image Processing*. Prentice Hall, 2007.

[22] M. Savvides, B. V. K. V. Kumar, and P. K. Khosla, "Eigenphases vs. eigenfaces," *Proc. Int'l Conf. Pattern Recognition*, vol. 3, pp. 810 – 813, 2004.

[23] D. B. Gennery, "Determination of optical transfer function by inspection of the frequency-domain plot," *J. Opt. Soc. Amer.*, vol. 63, pp. 1571 – 1577, 1973.

[24] M. Cannon, "Blind deconvolution of spatially invariant image blurs with phase," *IEEE Trans. Acoust. Speech Signal Process*, vol. ASSP-24, pp. 58 – 63, 1976.

[25] M. M. Chang, A. M. Tekalp, and A. T. Erdem, "Blur identification using the bispectrum," *IEEE Trans. Signal Processing*, vol. 39, no. 10, pp. 2323 – 2325, 1991.

[26] E. Oja, "Subspace methods of pattern recognition," *Research Studies Press*, 1983.

[27] S. Farsiu, M. D. Robinson, M. Elad, and P. Milanfar, "Fast and robust multiframe super resolution," *IEEE Trans. Image Processing*, vol. 13, no. 10, pp. 1327 – 1344, 2004.

[28] P. J. Phillips, H. Moon, P. J. Rauss, and S. Rizvi, "The feret evaluation methodology for face recognition algorithms," *IEEE Trans. Pattern Analysis and Machine Intelligence*, vol. 22, no. 10, pp. 1090 – 1104, 2000.

[29] P. J. Phillips, P. J. Flynn, T. Scruggs, K. W. Bowyer, J. Chang, K. Hoffman, J. Marques, J. Min, and W. Worek, "Overview of the face recognition grand challenge," *Proc. IEEE Conf. Computer Vision and Pattern Recognition*, vol. 1, pp. 947 – 954, 2005.

[30] T. Ahonen, A. Hadid, and M. Pietikainen, "Face description with local binary patterns: application to face recognition," *IEEE Trans. Pattern Analysis and Machine Intelligence*, vol. 28, no. 12, pp. 2037 – 2041, 2006.

[31] M. Turk and A. Pentland, "Eigenfaces for recognition," *J. Cognitive Neurosicence*, vol. 3, pp. 71 – 86, 1991.

[32] X. He, S. Yan, Y. Hu, and P. Niyogi, "Face recognition using laplacianfaces," *IEEE Trans. Pattern Analysis and Machine Intelligence*, vol. 27, no. 3, pp. 328 – 340, 2005.

[33] V. Ojansivu and J. Heikkila, "Blur insensitive texture classification using local phase quantization," *Proc. Int'l Conf. Image and Signal Processing*, pp. 236 – 243, 2008.